analytical chemistry

pubs.acs.org/ac Article

Macromolecular Orientation in Biological Tissues Using a Four-Polarization Method in FT-IR Imaging

Paulina Koziol, Danuta Liberda, Wojciech M. Kwiatek, and Tomasz P. Wrobel*

Cite This: *Anal. Chem.* 2020, 92, 13313−13318

Read Online

ACCESS | Metrics & More | Article Recommendations

ABSTRACT: Fourier transform infrared spectroscopy has emerged as a powerful tool for tissue specimen investigation. Its nondestructive and label-free character enables direct determination of biochemical composition of samples. Furthermore, the introduction of polarization enriches this technique by the possibility of molecular orientation study apart from purely quantitative analysis. Most of the molecular orientation studies focused on polymer samples with a well-defined molecular axis. Here, a four-polarization approach for Herman's in-plane orientation function and azimuthal angle determination was applied to a human tissue sample investigation for the first time. Attention was focused on fibrous tissues rich in collagen because of their cylindrical shape and established amide bond vibrations. Despite the fact that the tissue specimen contains a variety of molecules, the presented results of molecular ordering and orientation agree with the theoretical prediction based on sample composition and vibration directions.

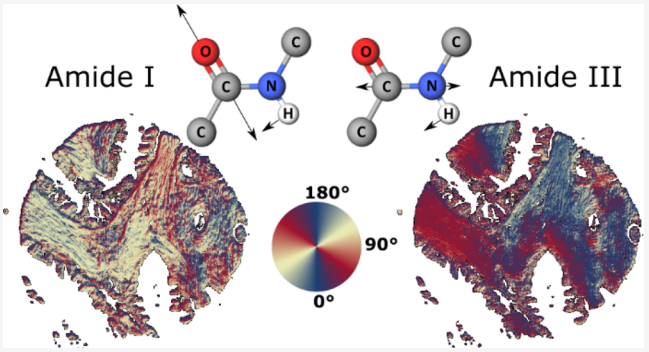

INTRODUCTION

Infrared (IR) spectroscopic imaging offers a wealth of information about the chemical composition of the sample in a spatially resolved manner, which is particularly attractive in biomedical applications.[1,2] However, structural aspects are still waiting to be incorporated into this modality.[3,4] Taking advantage of the anisotropic orientation of molecules in solid samples, it is possible to obtain different material responses when changing linear polarization of incoming IR light. Using this fact, the determination of molecular orientation with Fourier transform IR (FT-IR) was extensively explored, but mostly for polymer samples.[5,6] For example, polarized IR spectroscopy turned out to be an effective tool to examine the orientation and relaxation of drawn poly(ethylene terephthalate).[6−8] A more quantitative approach in the form of Herman's function with a two-polarization approach was used to determine the level of molecular ordering.[5,6,9,10] Later, a four-polarization method was proposed,[11−13] which gave a great tool for further polymer analysis,[14,15] especially when combined with imaging modalities.[12,13,16] A variety of other techniques may be used to determine molecular orientation: nuclear magnetic resonance, X-ray diffraction, polarized visible microscopy, fluorescence microscopy, second-harmonic generation (SHG), or Raman spectroscopy (RS).[17] However, each has specific requirements or drawbacks, such as a specific sample form (liquid or crystallized), lack of biochemical information, a complex instrumentation setup, or the need for labeling. Most of these can be met or outran with FT-IR imaging. A specimen of biological origin adds a level of difficulty to this approach, and among all FT-IR studies determining molecular orientation, only a few were focused on biological samples, especially tissues.[18−21] Although the most recent study used Stokes vector and a quantum cascade laser microscope to investigate fiber orientation in breast tissue surgical section,[22] that approach does not offer insights into vibrational mode orientation. This is especially challenging because a biological specimen contains a multitude of different molecules and deciphering contributions from each is a daunting task. However, the possibility of obtaining a vibrational mode-specific orientation map is very tempting and will open new avenues for research. So far, RS techniques are closest to reaching this goal, with a wealth of research done for tissue samples using coherent anti-Stokes Raman scattering (CARS) and stimulated Raman scattering (SRS) microscopy.[23,24] The differences in selection rules make FT-IR more sensitive to changes in the main molecular chain while RS to amino acid side chains. Furthermore, RS-based techniques are more sensitive to lipids while FT-IR to proteins. Another

Received: June 17, 2020
Accepted: August 28, 2020
Published: August 28, 2020

example of mapping method sensitive to vibrational modes is phase-sensitive vibrationally resonant sum-frequency generation (PSVR-SFG) microscopy derived from SHG—also used for tissue samples.[25] PSVR-SFG, CARS and SRS use relatively high power lasers to achieve specific vibrational transitions and are thus called discrete imaging techniques, while FT-IR measures the full spectrum and thus provides wide spectral information. Also, the use of lasers increases the risk of sample burn. On the other hand, the strength of CARS and SRS is the possibility to measure the second- and fourth-order parameter of the orientational distribution function, when FT-IR and PSVR-SFG can measure only the second-order parameter. Finally, FT-IR has an order of magnitude lower spatial resolution (in the far field) than the techniques based on visible light, which does not allow obtaining a high spatial detail but offers a large-scale sample coverage. Summing up, all techniques have their pros and cons and selection of a measurement method should be done including the sample type and targeted chemical information.

In this work, for the first time, we applied the four-polarization method to a human tissue (mainly fibrous and collagen-rich). The four-polarization approach allows obtaining unique information about the system—an in-plane orientation of dipole moment transitions (Herman's orientation function) along with the azimuthal angle.[11,12,16] Combining this computational method with FT-IR allows characterization of different vibrational modes.

MATERIALS AND METHODS

Sample Preparation and Measurements. A paraffin-embedded pancreatic tissue microarray (TMA) PA2072a was purchased from Biomax Inc. The TMA was sliced into 5 μm thick samples, one was placed on a regular glass and stained with hematoxylin and eosin (H&E) for histopathological inspection and the other was mounted on a BaF_2 salt plate for IR transmission measurements. The second sample was deparaffinized with 24 h hexane bath. Three tissue cores, later referred to as C1, D14, and J14 (Biomax naming convention), were selected for this research. All cores came from different patients with malignant ductal adenocarcinoma and were chosen because of high fibrous tissue content—adequate for molecular orientation study.

FT-IR measurements were performed in transmission mode with a Bruker Vertex 70v spectrometer coupled with a Hyperion 3000 microscope with 15× objective (2.7 μm projected pixel size, NA = 0.4) and a 64 × 64 FPA MCT detector. Two linear polarizers were inserted in default slots (first above the top objective and second under the bottom one) and were simultaneously rotated to remain in parallel to each other and obtain four target polarizations: 0, 45, 90, and 135°. Spectra were acquired from 3850 to 900 cm^{-1}, with an 8 cm^{-1} spectral resolution and a zero filling factor of 1. Sample and background signals were coaveraged 4 and 64 times, respectively. Furthermore, the stage was programmed to repeat the same positions for each polarization measurement, which led to four pixel-to-pixel spatially aligned data sets.

Data Preprocessing. To increase the spectral and spatial quality, data were denoised with the minimum noise fraction method, with 15 bands used for reconstructions.[26,27] Rubber-band baseline correction was applied, where each spectrum was divided into three segments: 3845−2750, 2746−1774, and 1770−900 cm^{-1}, determining ends for linear baseline subtraction. Specific band absorption was characterized by band integration rather than intensities for a single wavelength, which in our opinion provided a more stable outcome (results not shown).

Herman's Orientation Function and Azimuth Angle Theory. Anisotropic samples, such as polymers or fibers, absorb linearly polarized light to a different extent—depending on the polarization direction. Such an effect is called linear dichroism and is being often applied in the studies of molecular chain orientation. During IR absorption measurements with polarized light, if a specific band is to be observed, its dipole moment derivative must exhibit a nonzero component in the direction of light polarization. This is a condition for a band to be present in the spectrum. As a result, bands with dipole moments changing parallel to the polarization will appear as most intense, with the opposite situation for perpendicular bands.[28] A dichroic ratio was introduced to quantify this effect. It requires measurements with two orthogonal polarizations and is defined as[11,28]

$$D = \frac{A_{0^\circ}}{A_{90^\circ}} \tag{1}$$

where A_{0° and A_{90° are the absorbance for linear polarizations of 0 and 90°, respectively. On its own, this parameter provides information about the dipole moment orientation distribution with respect to the orientation axis but might also be employed in other parameter calculations.

A mathematical description of molecular orientation can be done utilizing orientation distribution function, which in the case of molecules with cylindrical symmetry is being approximated by a series of Legendre polynomials (with respect to the symmetry axis).[29] Depending on the mechanism of optical interaction, different measurement techniques can determine a different number of Lagrange polynomial coefficients.[29] FT-IR can provide a second-order coefficient,[29] which is also called Herman's orientation function or in-plane orientation function, calculated as[11,13]

$$f = \frac{D-1}{D+2}\frac{2}{3\cos^2\alpha - 1} \tag{2}$$

where D is the dichroic ratio and α is the angle between the transition dipole moment (of a specific absorption band) and the main molecular chain axis. The α angle needs to be defined individually for each absorption band; nonetheless, an approximation can be applied. If α is smaller than ≅54.73°, the band can be interpreted as parallel, whereas in the other case, the band can be interpreted as perpendicular. Herman's function f exhibits results in the range from −0.5 to 1, where −0.5 and 1 correspond to perfectly perpendicular and parallel bands, respectively. Reaching 0 indicates the isotropic character of a sample. However, 0 might also be obtained when polarization 0° forms a 45° angle with the main molecular axis (D = 1)—when two probing points are symmetrical on the sides of the cosine function. Such a result implies random orientation of a sample which, in fact, might be highly oriented. This matter was nicely discussed in the literature,[11] where an influence of 0 and 90° polarization direction on the in-plane orientation function was shown.

To aid this issue, a four-polarization method was developed, where a degree of molecular orientation can be determined independently from the choice of the direction of incident radiation polarization.[11,13] A simple formula to describe the absorbance A_γ under linearly polarized light was derived[11]

https://dx.doi.org/10.1021/acs.analchem.0c02591
Anal. Chem. 2020, 92, 13313−13318

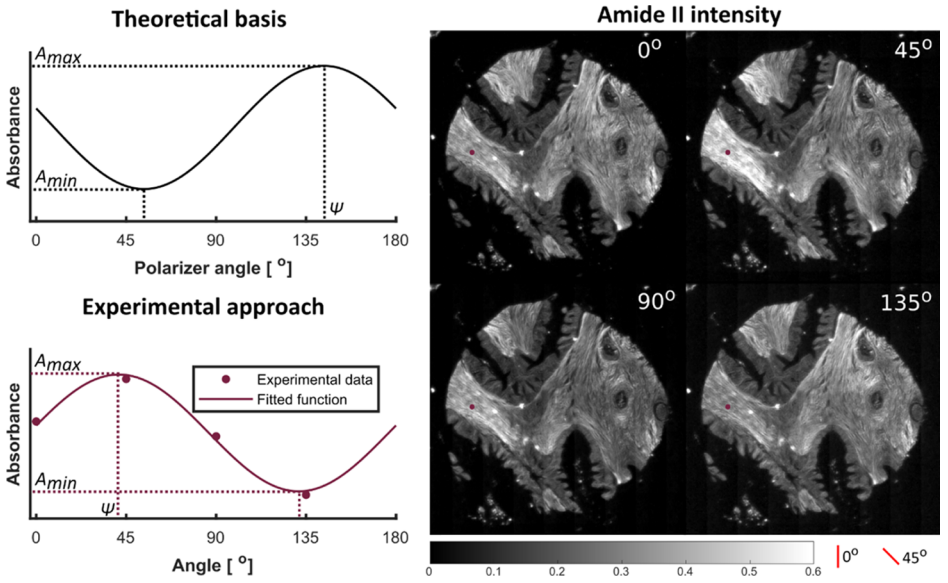

Figure 1. (Top left) Theoretical presentation of absorbance dependence from polarization. A_{max} and A_{min} correspond to the maximum and minimum absorption, respectively, and ψ represents the polarization when the absorbance reaches A_{max}. (Right) Intensity images of amide II absorbance under different polarizations. Purple dots indicate the pixel used for experimental approach demonstration. (Left bottom) Presentation of the experimental approach, where a cosine function indicated by equation 3 was fitted to absorbance for a single-pixel absorbance of amide II under four polarizations: 0, 45, 90, and 135°. Dashed lines are indicators of parameters of interest.

$$A_\gamma = \frac{A_{max} + A_{min}}{2} + \frac{A_{max} - A_{min}}{2}\cos 2(\gamma - \psi) \quad (3)$$

where A_{max} and A_{min} are the maximum and minimum absorbance, γ is a polarizer angle, and ψ is a polarizer angle when $A_\gamma = A_{max}$. This formula is graphically shown in the left top part of Figure 1, whereas visible differences in absorbance for four polarizations are presented on the right. This clearly shows how different regions of a sample are being highlighted when polarization matches the direction of a transition dipole moment. Different approaches of utilizing formula 3 were proposed,[11−13] with a nonlinear fitting method being preferred for this study. An exemplary calculation is shown in the left bottom part of Figure 1. Four experimental points describing absorbance under different polarizations (for a single pixel) are used as experimental results. The cosine function is later fitted allowing to find A_{max}, A_{min}, and ψ. This way, a new dichroic ratio might be determined in the form of

$$D_{max} = \frac{A_{max}}{A_{min}} \quad (4)$$

which, used for Herman's function calculation, provides results independent of the initial choice of orthogonal polarizer angles.

Another major source of information is delivered by the azimuthal angle ψ. This parameter points out polarization which, for a specific band, results in maximum absorption. In other words, polarization ψ is parallel to a transition dipole moment; therefore, it might be considered as a chemical bond direction or in-plane orientation indicator. An example is demonstrated in Figure 1, where purple dots in the right panel indicate pixel with absorbance plotted on the left side. The fitted curve shows ψ close to 45°, which agrees with the fact that this pixel comes from a region where the absorbance value was the highest for 45° polarization.

RESULTS AND DISCUSSION

As mentioned in the Materials and Methods section, samples with high fibrous tissue content were selected for this study to ease the interpretation. Histological images (H&E staining) of all three tissue sections are shown in the top part of Figure 2. Fibrous tissue with its cylindrical shape suits perfectly for molecular orientation studies. Moreover, high collagen content allows to determine the spectral regions and bands useful for this study. A single collagen molecule is built from three polypeptide chains, arranged into a helical conformation.[15,30] Therefore, three most important regions for FT-IR spectroscopic analysis are[15,18,30] amide I band (C═O stretching vibrations in the 1700−1600 cm^{-1} range), amide II band (C−N stretching and N−H bending vibrations in the 1590−1490 cm^{-1} range), and amide III band (N−H bending, C−N stretching, and C−H stretching vibrations in the 1290−1210 cm^{-1} range).

Herman's Function. Using eq 2 and amide III band integration, Herman's function was calculated for all pixels of the three tissue sections and results are presented in the middle part of Figure 2. The brightest regions indicate the areas with the highest molecular ordering. Comparing the images of in-plane orientation function with those of H&E shows that highly oriented regions origin mainly from fibrous tissues. Therefore, a random orientation is observed for epithelial cells and parts where fibers and cells are mixed together. Spectra from pixels with high and low (random) orientation were further investigated and are presented in the bottom part of Figure 2. The analysis of Herman's orientation function was carried out for amide III band (assuming $\alpha = 0°$) and spectral differences come to an agreement with what is being displayed above. Highly oriented pixels show significant differences between polarizations, while spectra from pixels with random orientation are almost overlapping in the amide III region. However, an interesting observation is that the same pixels that exhibit low orientation for the amide III band might show substantial differences for the amide I and II bands, as is shown

https://dx.doi.org/10.1021/acs.analchem.0c02591
Anal. Chem. 2020, 92, 13313−13318

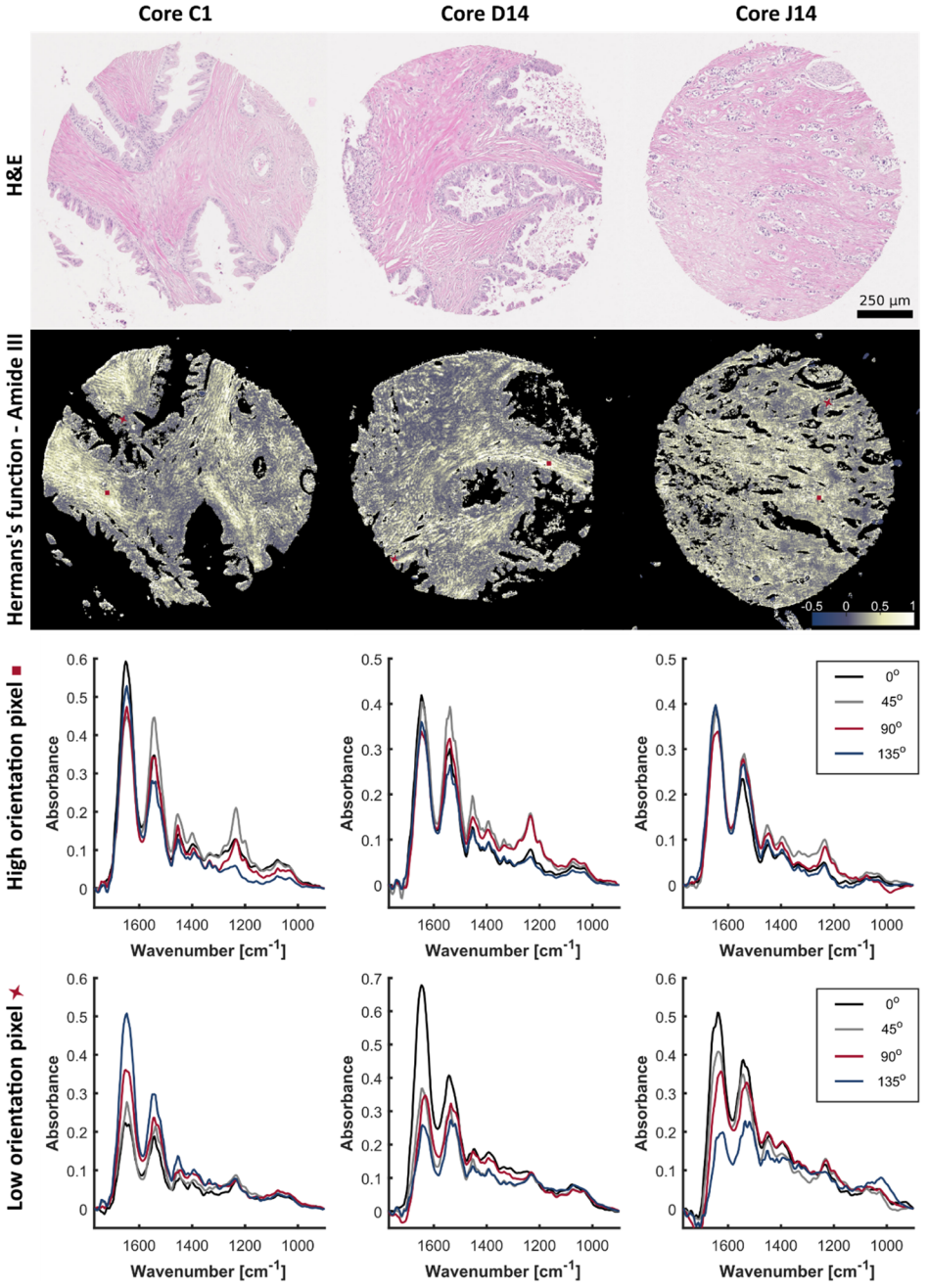

Figure 2. (Top row) Histological H&E stained image of samples. Pink regions are associated with fibrous tissues while purple with nuclei (cancerous cells). (Middle row) Herman's orientation function results calculated for amide III band integration. Red squares and crossed point pixels with high and low orientation, respectively. (Bottom) Spectra corresponding to pixels with a high and low orientation of amide III band. The pixels with low amide III band orientation were chosen to have at the same time high orientation of amide I band.

in the bottom spectra of Figure 2. The different behavior of spectral regions originating from the same protein contrast is very interesting. This implies different biomolecules contributing to the spectral signal in a distinct manner. Moreover, individual conformations of the same molecule may have unique ordering characteristics. To understand this spectral behavior, model systems of known composition will need to be investigated; however, it is very promising that such large differences can be observed in a biological, highly heterogeneous matrix.

Azimuthal Angle. An azimuthal angle ψ describes the in-plane orientation of specific molecular bonds, or being more specific, the direction of transition dipole moment. The results for amide I, amide II, and amide III of all three samples are presented in Figure 3. The results span from 0 to 180° because of the fact that phase shifting by π gives the same results. A circular chart representing color-angle correspondence is shown in Figure 3. The most interesting feature to be inspected is the main molecular chain axis (fiber direction), which was observed in histological images (Figure 2). Amide II and amide III results in Figure 3 show a very similar outcome for all three samples. Observed angles come to a complete agreement with fiber structure in H&E images. The explanation of this comes from analyzing the type of vibrations involved in amide II and amide III spectral regions. Both include C−N stretching and N−H bending vibrations, which

https://dx.doi.org/10.1021/acs.analchem.0c02591
Anal. Chem. 2020, 92, 13313−13318

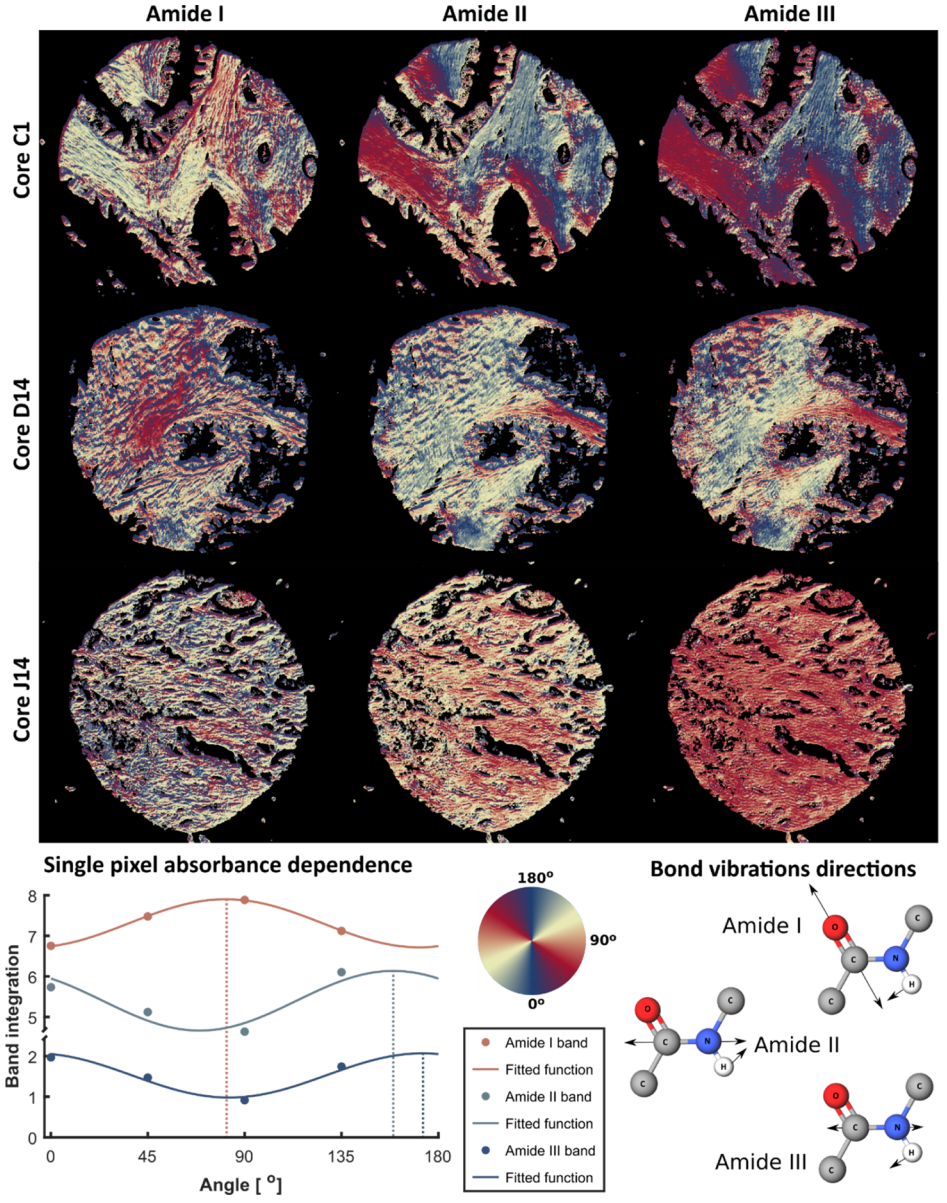

Figure 3. (Top) Orientation of amide I, amide II, and amide III bands represented by the azimuthal angle ψ. (Bottom left) Absorbance dependence from polarization for three analyzed spectral regions, for a single pixel from core C1. (Bottom right) Theoretical representation of amide bond vibration directions.

are present in collagen polypeptide chains. Especially, stretching of the C−N bond might be a great indicator of the main molecular chain orientation of collagen. The spatial sensitivity of this method is particularly visualized by C1 core results, with fibers changing directions throughout the whole sample. Furthermore, one of the most interesting observations is that the spatial orientation coming from amide I band is almost perpendicular to that of amide II and amide III bands, as predicted by the theoretical models of bond vibration directions. Absorbance dependence from the polarization of all the three spectral regions was plotted for a single pixel from core C1. The results are shown at the bottom of Figure 3. This plot is color-coded, so each series color corresponds to a pixel color in the top image. It is clear that the maximum absorbance (indicated by the dashed line) is shifted by ∼90° for amide II and amide III, with respect to amide I. Another strong feature of this method is pointed out by the results of orientation for epithelial regions—which were found to be mostly random. This is caused by the lack of collagen or other molecules with the oriented amide III band. However, random orientation might also be achieved by collagen in two specific cases: first, when fiber direction is parallel to the optical axis—perpendicular to the focal plane and second, when bundles of fibers exhibiting different values of the azimuthal angle meet at one point and are below the spatial resolution capabilities of the system.

These examples show that even in a complex biological matrix containing multiple components, it is possible to observe macromolecular ordering. Moreover, the four-polarization method enables vibration-specific observation of spatially resolved orientation of dipole moment transitions. This opens up a new area of research, not only focused on polymers but also on naturally occurring macromolecules.

https://dx.doi.org/10.1021/acs.analchem.0c02591
Anal. Chem. 2020, 92, 13313−13318

CONCLUSIONS

The field of spatially resolved IR polarimetry is rapidly expanding, and more advanced approaches allow the identification of new structural parameters in addition to just chemical composition. The first application of the four-polarization method to human tissue showed that calculating Herman's orientation function and obtaining the azimuthal angle of selected vibrational modes is feasible and opens up new avenues in studying biological materials.

AUTHOR INFORMATION

Corresponding Author

Tomasz P. Wrobel − *Solaris National Synchrotron Radiation Centre, Jagiellonian University, Krakow 30-392, Poland; Institute of Nuclear Physics, Polish Academy of Sciences, Krakow PL-31342, Poland;* orcid.org/0000-0003-2053-0570; Email: tomek.wrobel@uj.edu.pl

Authors

Paulina Koziol − *Solaris National Synchrotron Radiation Centre, Jagiellonian University, Krakow 30-392, Poland; Institute of Nuclear Physics, Polish Academy of Sciences, Krakow PL-31342, Poland*

Danuta Liberda − *Solaris National Synchrotron Radiation Centre, Jagiellonian University, Krakow 30-392, Poland; Institute of Nuclear Physics, Polish Academy of Sciences, Krakow PL-31342, Poland*

Wojciech M. Kwiatek − *Institute of Nuclear Physics, Polish Academy of Sciences, Krakow PL-31342, Poland;* orcid.org/0000-0002-2197-8572

Complete contact information is available at: https://pubs.acs.org/10.1021/acs.analchem.0c02591

Notes

The authors declare no competing financial interest.

ACKNOWLEDGMENTS

This research was supported by the National Science Centre, Poland ("three-dimensional macromolecule orientation by means of IR imaging and its significance in cancer micro-environment", grant no. 2018/31/D/ST4/018). This research was performed using the equipment purchased in the frame of the project cofunded by the Malopolska Regional Operational Program Measure 5.1 Krakow Metropolitan Area as an important hub of the European Research Area for 2007−2013, project no. MRPO.05.01.00-12-013/15. The authors declare no conflicts of interest.

REFERENCES

(1) Wrobel, T. P.; Mateuszuk, L.; Kostogrys, R. B.; Chlopicki, S.; Baranska, M. *Analyst* **2013**, *138*, 6645−6652.
(2) Walsh, M. J.; Reddy, R. K.; Bhargava, R. *IEEE J. Sel. Top. Quantum Electron.* **2012**, *18*, 1502−1513.
(3) Wrobel, T. P.; Bhargava, R. *Anal. Chem.* **2018**, *90*, 1444−1463.
(4) de los Santos Pereira, A.; Cernescu, A.; Svoboda, J.; Sivkova, R.; Romanenko, I.; Bashta, B.; Keilmann, F.; Pop-Georgievski, O. *Anal. Chem.* **2020**, *92*, 4716−4720.
(5) Everall, N. J.; Chalmers, J. M.; Local, A.; Allen, S. *Vib. Spectrosc.* **1996**, *10*, 253−259.
(6) Lu, X.; Hay, J. N. *Polymer* **2001**, *42*, 8055−8067.
(7) Branciforti, M. C.; Silva, L. B.; Bretas, R. E. S. *J. Appl. Polym. Sci.* **2006**, *102*, 2241−2248.
(8) Duchesne, C.; Kong, X.; Brisson, J.; Pézolet, M.; Prud'homme, R. E. *Macromolecules* **2002**, *35*, 8768−8773.
(9) Albunia, A. R.; Di Masi, S.; Rizzo, P.; Milano, G.; Musto, P.; Guerra, G. *Macromolecules* **2003**, *36*, 8695−8703.
(10) Albunia, A. R.; Musto, P.; Guerra, G. *Polymer* **2006**, *47*, 234−242.
(11) Hikima, Y.; Morikawa, J.; Hashimoto, T. *Macromolecules* **2011**, *44*, 3950−3957.
(12) Hikima, Y.; Morikawa, J.; Hashimoto, T. *Macromolecules* **2012**, *45*, 8356−8362.
(13) Hikima, Y.; Morikawa, J.; Hashimoto, T. *Macromolecules* **2013**, *46*, 1582−1590.
(14) Ryu, M.; Balčytis, A.; Wang, X.; Vongsvivut, J.; Hikima, Y.; Li, J.; Tobin, M. J.; Juodkazis, S.; Morikawa, J. *Sci. Rep.* **2017**, *7*, 7419.
(15) Riaz, T.; Zeeshan, R.; Zarif, F.; Ilyas, K.; Muhammad, N.; Safi, S. Z.; Rahim, A.; Rizvi, S. A. A.; Rehman, I. U. *Appl. Spectrosc. Rev.* **2018**, *53*, 703−746.
(16) Wrobel, T. P.; Mukherjee, P.; Bhargava, R. *Analyst* **2017**, *142*, 75−79.
(17) Cheng, J.-X.; Xie, X. S. *Science* **2015**, *350*, aaa8870.
(18) Camacho, N. P.; West, P.; Torzilli, P. A.; Mendelsohn, R. *Biopolymers* **2001**, *62*, 1−8.
(19) Hsu, W.-L.; Davis, J.; Balakrishnan, K.; Ibn-Elhaj, M.; Kroto, S.; Brock, N.; Pau, S. *Opt. Express* **2015**, *23*, 4357.
(20) Choi, J.-H.; Cho, M. *J. Phys. Chem. B* **2014**, *118*, 12837−12843.
(21) Miller, L. M.; Dumas, P. *Biochim Biophys Acta* **2006**, *1758*, 846−857.
(22) Phal, Y.; Yeh, K. L.; Bhargava, R. Polarimetric Infrared Spectroscopic Imaging Using Quantum Cascade Lasers. *Advanced Chemical Microscopy for Life Science and Translational Medicine*; SPIE, 2020; p 1125210.
(23) Duboisset, J.; Berto, P.; Gasecka, P.; Bioud, F.-Z.; Ferrand, P.; Rigneault, H.; Brasselet, S. *J. Phys. Chem. B* **2015**, *119*, 3242−3249.
(24) de Vito, G.; Bifone, A.; Piazza, V. *Opt. Express* **2012**, *20*, 29369.
(25) Han, Y.; Raghunathan, V.; Feng, R.-r.; Maekawa, H.; Chung, C.-Y.; Feng, Y.; Potma, E. O.; Ge, N.-H. *J. Phys. Chem. B* **2013**, *117*, 6149−6156.
(26) Koziol, P.; Raczkowska, M. K.; Skibinska, J.; Urbaniak-Wasik, S.; Paluszkiewicz, C.; Kwiatek, W.; Wrobel, T. P. *Sci. Rep.* **2018**, *8*, 14351.
(27) Raczkowska, M. K.; Koziol, P.; Urbaniak-Wasik, S.; Paluszkiewicz, C.; Kwiatek, W. M.; Wrobel, T. P. *Anal. Chim. Acta* **2019**, *1085*, 39−47.
(28) Griffiths, P. R.; De Haseth, J. A. *Fourier Transform Infrared Spectrometry*; Wiley-Interscience, 2007.
(29) Lee, Y. J. *Opt. Express* **2018**, *26*, 24577.
(30) Belbachir, K.; Noreen, R.; Gouspillou, G.; Petibois, C. *Anal. Bioanal. Chem.* **2009**, *395*, 829−837.